Nanoscale

Accepted Manuscript

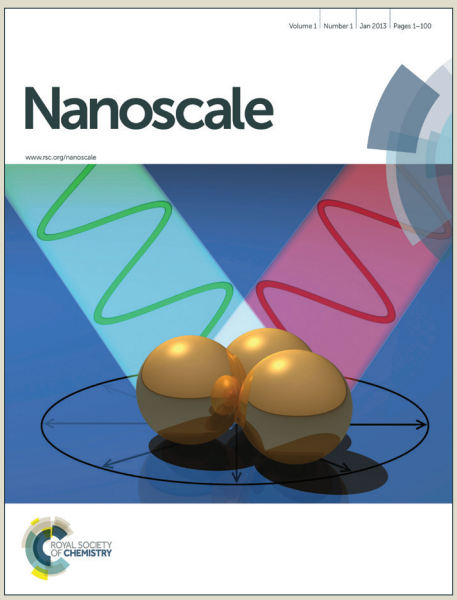

ROYAL SOCIETY OF CHEMISTRY

www.rsc.org/nanoscale

Cite this: DOI: 10.1039/c0xx00000x

www.rsc.org/xxxxxx

ARTICLE TYPE

Platinum nanoparticles on electrospun titania nanofibers as hydrogen sensing material working at room temperature

Ilaria Fratoddi,[ab] Antonella Macagnano,[c] Chiara Battocchio,[d] Emiliano Zampetti,[c]* Iole Venditti,[a]* Maria V. Russo[ae] and Andrea Bearzotti[c]

The authors contributed equal to both experiments and manuscript preparation.

Received (in XXX, XXX) Xth XXXXXXXXX 20XX, Accepted Xth XXXXXXXXX 20XX
DOI: 10.1039/b000000x

Platinum nanoparticles (PtNPs), with diameters of 3-10 nm, were synthesized by water phase reduction, using 3-mercapto-1-propanesulfonate (3MPS) as hydrophilic capping agent. PtNPs were deposited by dipping on titania nanofibers (TiO_2NFs), obtained by electrospinning. The investigated properties of the Pt-TiO_2 hybrid at room temperature show that this material combines the properties of photoconduction of titania and the photocatalytic activity of the hybrid. To assess the best performance of Pt-TiO_2, different measurements were performed at room temperature, comparing hydrogen response under UV of the uncoated TiO_2NFs, compared with the Pt-TiO_2 system prepared with two different amount of PtNPs. During the sensing tests toward hydrogen an enhancement of photoconductivity (150%), an increase in response (400%) and an overall improvement of their dynamic behaviour were observed.

1. Introduction

Nanostructured materials are particularly interesting due to their high surface area-to-volume ratio and synergetic effects, which are promising for energy,[1,2,3] medicine,[4,5] optics,[6,7,8] biological,[9,10,11] and sensing applications.[12,13,14,15] In this framework, metal nanoparticles play a leading role because of the peculiar properties of the nanostructures, combined with semiconductivity and catalytic activity, thus making them relevant in both scientific research and industrial applications.[16,17,18,19] Among others, platinum nanoparticles (PtNPs) are exploited to achieve innovative hybrid nanostructures for enhancing gas sensitivity, hydrogen response and for energy applications, where the nanodimensions allow to increase the surface properties and, at the same time, reduce metal amount and costs.[20,21,22] The operating temperature is another important issue for several applications, especially for sensors.[23,24] A room-temperature sensor could simplify device design by eliminating the heater component. Moreover, this feature allows to save electrical power and to assemble the sensor on flexible polymer substrates, and most importantly, avoid danger of explosions.[25,26] To date, it has been experimentally proven that metallic catalysts such as Ag,[27] Au,[28] Pd,[29,30] and Pt[31] nanoparticles, loaded onto the surfaces of the oxide supports, serve as surface activators, promoting the dissociative adsorption of H_2 which is an important step in the surface reaction. Therefore, it could be expected that a promising room-temperature hydrogen sensor may be obtained by combining metal oxides and noble-metal nanoparticles.[32] It should be noted that the preparation processes could require high temperature and multi step synthetic routes.[33] One of the goals in this field will be to combine the chemicals with an easy, safe, readly scaled up and low cost procedure.

Titanium dioxide (TiO_2) is a widely used material in both research and industrial fields, due to its inherent chemical stability, transparency, low cost, and minimal toxicity.[34,35,36] Several applications have been developed for devices based on nanostructured titania obtained by electrospinning,[37,38] due to its photocatalytic, photoconductive and wetting properties.[39] Nanostructured composites based on titania and metal nanoparticles have been exploited as well.[40,41,42]

In this work we have investigated the properties of titania nanofibers (TiO_2-NFs) decorated with PtNPs giving the hybrid Pt-TiO_2, upon interacting with hydrogen at room temperature. Experimental results have pointed out that Pt-TiO_2 combines the properties of photoconduction of titania with the sensitivity of platinum to H_2, and is particularly promising when interacts with hydrogen in the range of 100-1150 ppm, under UV and at room temperature.

2. Experimental Part

Materials

Potassium tetracloroplatinate (K_2PtCl_4, Aldrich, 98.5%), sodium borohydride ($NaBH_4$, Aldrich, 99%), and sodium 3-mercapto-1-propanesulfonate (3MPS, $C_3H_7S_2O_3Na$ Aldrich, 98%), were used as received. Deionized water was obtained from Zeener Power I Scholar-UV (electrical resistivity 18.2 MΩ). Argon flux was flown through the reaction solvents for the deoxygenation of the

reaction mixtures. A solution of polyvinylpyrrolidone (PVP, Aldrich, 21,300,000 uma) in anhydrous ethanol (EtOH, Aldrich) with a 1:4 (w/v) solution of titanium isopropoxide (TiiP, Aldrich 98%), a 1:1 (v/v) mixture of glacial acetic acid (Aldrich) and EtOH, was used as TiO_2 nanofibers precursor.

PtNPs Synthesis

The synthesis of the PtNPs was performed at room temperature, through a redox reaction in aqueous phase starting from a K_2PtCl_4 water solution with $NaBH_4$ and using 3MPS as capping agent. The reactions were run with different Pt/S molar ratios, as reported in ESI (table 1). The typical procedure for the synthesis of Pt-3MPS-4 is reported below, as an example. K_2PtCl_4 (0.200 g, $4.8 \cdot 10^{-4}$ mol) was dissolved in 16 mL of deionized H_2O at pH = 2 and subsequently a solution of 3MPS (0.021 g, $1.2 \cdot 10^{-4}$ mol) in 20 mL of H_2O was poured into the same reaction vessel at room temperature, under vigorous stirring. The yellow solution was degased by bubbling Argon for 10 min. $NaBH_4$ (0.177 g, $4.8 \cdot 10^{-3}$ mol) dissolved in 10 mL of deionized H_2O was added to the reaction mixture by slow drop wise addition (lasted 30 minutes), using a syringe. The reaction mixture was left at room temperature under stirring for 20 hours. The brown crude reaction products were subjected to dialysis, in distilled water for 5 days, and then the purified PtNPs have been characterized by means of UV-Vis, FTIR DLS and ζ-potential. Characterization data are herein reported for Pt-3MPS-4 as an example. DLS ($2R_H$[nm], H_2O): 20 ± 5.0; IR (ν [cm^{-1}], nujol): 1165, 1061, 598 ν(SO_3^-); 322 e 350 cm^{-1}(Pt-S); ζ-Potential ([mV], H_2O): -35; yield 65%.

TiO_2NFs preparation

A titania nanofibrous layer was fabricated by the electrospinning technique.[43] Electrospinning uses an electrical charge to draw nanofibers from a polymer solution. Such a deposition technique allows the fabrication of the titania nanofibrous scaffold directly on the sensor transducer minimizing the substrate adhesion issues.[44] The TiO_2-NFs preparation consisted of two main steps. The first one was the deposition of the nanofibrous layer composed of a TiO_2 precursor polymer. The latter step was a thermal treatment to remove the organic material and to allow the nanofibers crystallization, according to literature.[45]

In detail, by mixing a solution of PVP in anhydrous ethanol with a 1:4 (w/v) solution of titanium isopropoxide in a 1:1 (v/v) mixture of glacial acetic acid and EtOH, the TiO_2 precursor (Tiip/PVP) was obtained.[46] The polymer solutions were prepared in a glove box (5% RH) and stirred for 3 hours at room temperature. 2.0 mL of precursor solution was put in a glass syringe equipped with a stainless steel needle (inner tip diameter = 480 μm). An electrical potential of 6 kV (direct current mode) was applied to the needle, the rotating collector and IDE were connected to ground. During the electrospinning process the solution feeding rate was controlled by a syringe pump controller (KDS 200, KD Scientific). The nanofibers were collected on a set of substrates mounted on a rotating metal collector 15 cm far from the syringe. The deposition was performed setting the syringe feed rate at 100 μL/h and 500 rpm as the collector speed. The deposition, lasting 20 min, was carried out in a controlled box at 24°C and at 45 % of RH. The following step, after the production of Tiip/PVP nanofibers in sol–gel form, was the calcination process to remove the organic material and to obtain TiO_2-NFs having nanocrystalline form. The thermal treatment was carried out in air using a controlled furnace, where the temperature was increased from 25°C to 550°C with a rate of 1°C/min. The material was maintained at 550°C for 4 h to complete the crystallization processes. After that, the temperature was decreased to 25°C within 6 h.

Pt-TiO_2 preparation

Two water suspensions of Pt-3MPS-4 have been used to be absorbed on TiO_2-NFs: 400 μg/mL and 800 μg/mL. Dip-coating technique was used to deposit the nanoparticles on the nanofibrous layer. The withdrawal speed of the substrate (covered by nanofibers) from the solution was adjusted at 10 mm/min. The deposition was performed in a closed chamber filled with synthetic air and the humidity and temperature were maintained at 40% RH and 23°C respectively. Finally, the samples were placed in a controlled oven at 37°C overnight. In particular three different devices were prepared: the first one with TiO_2-NFs dipped in 400 μg/ml (device D1), the second with TiO_2-NFs dipped in 800 μg/ml (device D2) and the last one with TiO_2-NFs alone (D0).

Instruments

Absorption spectra of PtNPs dispersed in deionized water were measured in 1.00 cm optical path quartz cells by using a Cary 100 Varian spectrophotometer. FT-IR and FIR spectra were recorded with a Bruker Vertex 70 instrument using KRS-5 cells, in the range 4000-400 cm^{-1} and 400-200 cm^{-1}, respectively; the samples have been prepared as nujol mulls. FE-SEM images and EDX data have been acquired with the Auriga Zeiss instrument (resolution 1 nm, applied voltage 6-12 kV) on drop casted films on metallic holder, from water solution. Malvern Zetasizer Nanoseries instrument (Malvern, UK) equipped with a 10 mW HeNe laser at a 632.8 nm wavelength was used to run Dynamic Light Scattering (DLS) measurements on the PtNPs aqueous suspensions (0.2 mg/mL) at a T= 25.0 ± 0.2°C. The Correlation functions were collected at θ = 90° relative to the incident beam, and delay times from 0.8 μs to 10 s were explored. Non-negative least-squares (NNLS)[47] or CONTIN[48] algorithms, supplied with the instrument software, were used to fit correlation data. The average hydrodynamic radius of the diffusing objects was calculated, as reported in previous works.[49,50,51] The ζ-potential was calculated from the measured electrophoretic mobility by means of the Smolukovsky equation.[52,53] The morphology of the materials was investigated through atomic force microscopy analysis (AFM). All the measurements were performed in non-contact mode with a PSIA XE 100 NC-HR instrument by observing samples deposited on interdigitate electrodes (IDE), prepared as reported in the next paragraph. The molecular and electronic structure of pristine PtNPs and PtNPs deposited onto TiO_2 nanofibres, as well as TiO_2-NF itself, were probed by x-ray photoelectron spectroscopy (XPS). XPS analysis was performed in an instrument of our own design and construction, consisting of a preparation and an analysis UHV chamber, (resolution of 1.0 eV as measured at the Ag 3d5/2 core level). MgKα non-monochromatised X-ray radiation (1253.6 eV) was used for acquiring core level spectra of all samples (C1s, S2p, Pt4f, Ti2p,

Na1s and O1s). The spectra were energy referenced to the C1s signal of aliphatic C atoms having a binding energy BE = 285.00 eV. Atomic ratios were calculated from peak intensities by using Scofield's cross section values and calculated λ factors.[54] Curve-fitting analysis of the C1s, S2p, Pt4f, Ti2p, Na1s and O1s spectra was performed using Voigt profiles as fitting functions, after subtraction of a Shirley-type background.[55]

Sensing measurements

The interaction between hydrogen and Pt-TiO_2 has been studied measuring the changes of its photo conductivity. The nanomaterial photoconduction effect was revealed by interdigitate electrodes (IDE) working as a transducer. IDE consisted of 40 pairs of platinum electrodes with a gap of 20 µm, 100 nm thick and 20 µm width, implemented on a passivated silicon substrate (8 x 9 x 0.4 mm).[56,57] A set of IDE was positioned on the electrospinning collector to deposit the TiO_2 precursor nanofibers. Subsequently, the fibres were thermally treated to perform the calcination process[38] and then coated with Pt nanoparticles by dip-coating process as previously described. The devices were placed in a measurement chamber made of stainless steel. Ultraviolet light emitting diode (UV LED, LZ1-00U600, λ = 365 nm, PUV = 8 mW/cm^2, by LED ENGIN) was used to irradiate the devices during all the measures. The LED was placed on the top of the chamber where a quartz window allowed the light to pass, preserving the sealing. Responses were recorded measuring the current (I_D) at a fixed voltage polarization (V_D = 1 V) by Keithley 595 quasi static C/V meter. A gas delivery system, consisting of a set of mass flow controllers (MKS 147B) was used to generate controlled hydrogen concentration in nitrogen carrier. A cylinder of 10000 ppm of H_2 (SIAD, Praxair) diluted in nitrogen has been used. The measurements were performed at 25°C and at 200 sccm (standard cubic centimetres per minute) of total gas flow and in dry condition. In order to avoid material degradation we have fixed at 120 s the exposure to hydrogen while the recovery phase (cleaning) was performed in nitrogen with an exposure time of 360 s.

3. Results and discussion

PtNPs were obtained by a wet redox procedure; by varying the Pt/thiol molar ratio, monodispersed and stable particles with sizes in the range 3-10 nm, were isolated. FE-SEM, DLS and ζ-potential measures, reported in Table 1 (see ESI for details) confirmed the size and water stability of the colloidal system.

Table 1. FE-SEM DLS and ζ-potential data of PtNPs

Sample ID	FE-SEM diameter (nm)	DLS diameter (nm)	ζ -potential (mV)
Pt-3MPS-1	5 ± 3	7 ± 3	-30
Pt-3MPS-2	5 ± 3	12 ± 3	-32
Pt-3MPS-3	7 ± 3	15 ± 3	-32
Pt-3MPS-4	10 ± 5	20 ± 5	-35

It can be noticed that the dimensions obtained from DLS are often bigger than those obtained from FE-SEM images, since DLS measures the hydrodynamic radius. It is well known that the colloidal particles dispersed in aqueous environment undergo a certain effect of swelling and this behaviour is typical for hydrophilic nanoparticles.[58] Because the synthesized PtNPs have a surface charge given by the sulfonate group, the ζ-potential measurements give information on their surface charge and their stability. The measured ζ-potential is of practical interest to assess the dispersion stability, because it determines the inter-particle forces.[59,60] High values of zeta potential (<-30 mV or > +30 mV) indicate that the nanoparticles remain far apart, due to the repulsion between the charges that makes them stable in suspension.[61] In fact, several tests performed on our samples, have shown high degree of hydrophilicity during the time: the same ζ-potential values were obtained for the PtNPs that have high stability in water solution up to 6 months at room temperature, in particular Pt-3MPS-4 with ζ-potential -35 mV. This sample has been chosen for the preparation of the hybrid due to its higher stability during the time (up to 1 year). Moreover, the best yield of this sample makes it the most promising for a possible technology transfer.

FTIR spectrum of PtNPs shows the presence of the bands associated to the stretching of the SO_3^- group, at about 1170 cm^{-1}, 1055 cm^{-1}, 600 cm^{-1}, which confirms the presence of the 3MPS on the surface of the NPs. Attention was then addressed to the IR spectrum at low frequencies (FIR) for the identification of the bands characteristic of the Pt-S stretching at 322, 350 cm^{-1} and 450 cm^{-1}, which assess the presence of the covalent Pt-S bond. From the UV-Vis spectra of PtNPs in water suspension (see ESI) an absorption curve appears with maximum at 264 nm, similar to that observed by Yee et al. for Pt particles stabilized with octadecanthiol.[62]

The PtNPs were loaded on the TiO_2-NFs electrodeposited on IDE and the resulting composites were characterized before the sensing tests. Three different devices were prepared: D1 and D2 obtained by dipping the TiO_2-NFs in the two described solution having different concentration of PtNPs and D0 *i.e.* TiO_2 nanofibers alone, as a comparison.

The surface morphology and composition of D2 has been studied by FE-SEM and EDX. In Figure 1ab, small PtNPs are observed on the TiO_2-NFs deposited on the IDE: the grains visible at the intersection of the fibers are due to PtNPs, mechanically locked between the fibers during the dipping, as confirmed by the EDX analysis.

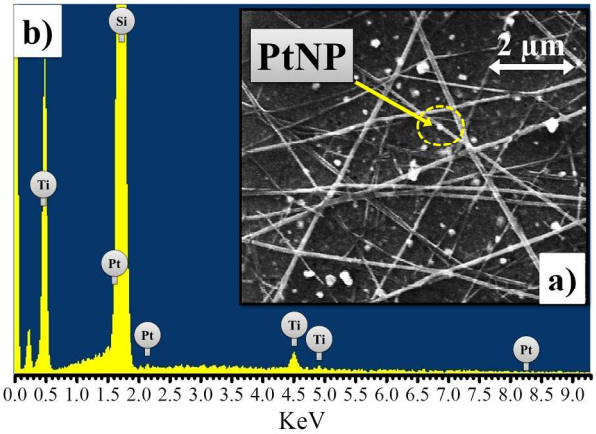

Figure 1. Characterization of D2: a) FESEM image; b) EDX.

Figure 2 depicts the AFM image analysis of TiO_2-NF and hybrid TiO_2-NF decorated with PtNPs (D2) on SiO_2 substrate: TiO_2-NF (Figure 2a) exhibits an average diameter of 80 nm and the Pt-TiO_2 hybrids, D2, (Figure 2b) points out the presence of PtNPs on the nanofibers surface. The sensing activity of Pt toward H_2 is a topic of interest for the development of hydrogen sensors and has been investigated both in the past by Lewis[63,64] and more recently by groups that produce hetero-nanostructures.[65,66]

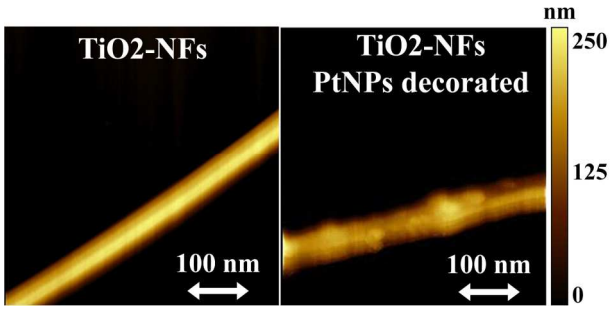

Figure 2. AFM images of (a) TiO_2-NF and (b) Pt-TiO_2 hybrid system (D2).

D1, D2 were also characterized by means of x-ray photoelectron spectroscopy, as to acquire information about the electronic and chemical structure of the functionalized nanoparticles on the devices surface. For comparison, measurements were also performed on pristine PtNPs and TiO_2-NFs. C1s, S2p, O1s, Na1s, Pt4f, Ti2p core level signals were acquired, and the complete Binding Energy (BE), full width half maxima (FWHM) and atomic percent values, together with the features assignments, are summarized in ESI 5. The most indicative signals to achieve information about the 3MPS molecule and metallic cluster are S2p and Pt4f. Pt4f spectrum of D2 (Figure 3a) appears structured, and by following a peak-fitting procedure two pairs of spin-orbit components can be individuated. The first feature (Pt4f7/2 BE = 71.2 eV) is associated to metallic Pt, and is due to platinum atoms in nanoparticles bulk [67]; the spin-orbit pair at higher BE values ($Pt4f_{7/2}$ = 72.5 eV BE) is indicative for positively charged Pt atoms, as expected for surface atoms bonded to sulphur.[67] It is noteworthy that the pristine PtNPs sample shows exactly the same features, with a fully reproducible intensity ratio (ESI 5), thus suggesting that the capped nanoparticle electronic structure (and activity) is preserved in the device. S2p spectra provide complementary information about the chemical bond between thiolates and surface platinum atoms of PtNPs. As shown in Figure 3b for D2 sample, S2p signals are also composite, showing a pair of spin-orbit components at BE values indicative for thiol-like sulphur atoms covalently bonded to metals ($S2p_{3/2}$ BE = 161.5 eV), [68,69] and a second spin-orbit doublet at higher BE values ($S2p_{3/2}$ BE = 166 eV) associated to the $–SO_3^-$ moieties of 3-MPS molecules. The intensity ratio between the two kinds of S atoms is close to 1/1, as expected from the molecular structure, supposing that all 3-MPS molecules are covalently bonded to Pt atoms. Indeed, physisorbed thiols would give rise to S2p peaks at about 164 eV BE ($S2p_{3/2}$) [70], associated to "free" thiol moieties, that are not observable in D2 (nor in D1) spectrum.

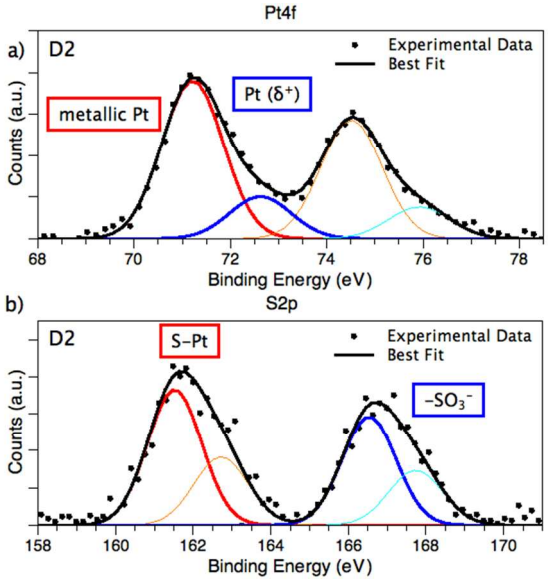

Figure 3. S2p and Pt4f spectra collected on sample D2; the two S2p signals, corresponding to sulphur atoms bonded to Pt and $-SO_3^-$ moieties respectively, are in about 1/1 atomic ratio. Pt4f signals are also indicative of Pt atoms in two different electronic states: the main signal (red - orange) is attributed to metallic platinum (NPs "core" Pt atoms); the blue - cyan spin-orbit pair is indicative for positively charged Pt atoms (and attributed to Pt atoms bonded to thiol on NPs surface).

XPS data acquired at the Ti2p core level showed a chemical shift in D1 and D2 samples, with respect to the pristine TiO_2-NFs system. For TiO_2-NFs we observe a $Ti2p_{3/2}$ component BE value of 458.55 eV, in excellent agreement with the value expected for titanium dioxide (458.60 eV);[67] Ti2p signal of D2 and D1 samples appear shifted at higher BE values of about 1eV in samples D1 and D2 ($Ti2p_{3/2}$ BE = 459.51 eV; 459.43 eV respectively), as evidenced in the following Figure4.

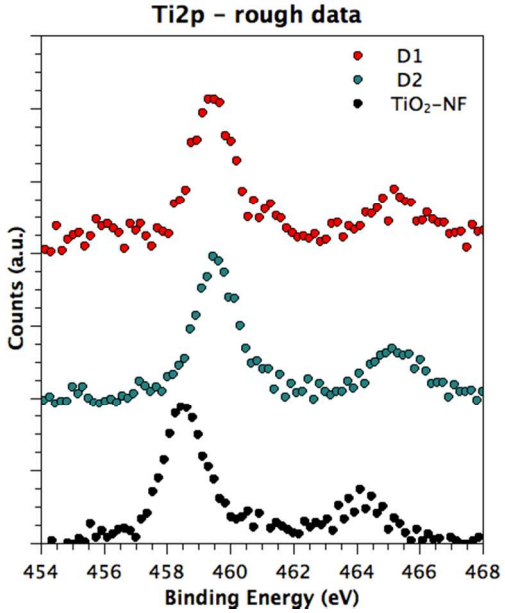

Figure 4. Rough experimental data collected on D1, D2 and TiO_2-NFs at Ti2p core level. D1 and D2 spectra appear shifted at higher BE values.

We have studied the improvement offered by the presence of PtNPs in the interaction of TiO_2-NFs toward H_2. The D1, D2, and D0 devices have been tested to investigate their response to hydrogen. First we have measured the current versus the applied voltage (Figure 5), in a stream of dry nitrogen and in presence of UV irradiation, to advantage of the properties of photoconduction of titania.[38] The current versus voltage curves present a non linear trend due to the presence of a Schottky barrier potential ($|V_D|$ = 0.6 V) between the titania and electrodes (IDE/TiO_2/IDE).[71,72] The PtNPs arranged on nanofiber surface, connect the fibres, increasing the overall device conductance. The I/V curves point out that the conductance of the devices (D1, D2) increase with increasing particle concentration: D2 curve is upper than D1 and D0 curves. Without the UV irradiation (λ=365 nm, P_{UV} = 8 W/cm^2) the measured current of the three devices was more than three order of magnitude lower than the measured current under UV irradiation. For example, in the case of TiO_2-NF the current intensity changed form 20 pA to 12 µA (at V_D=1 V).

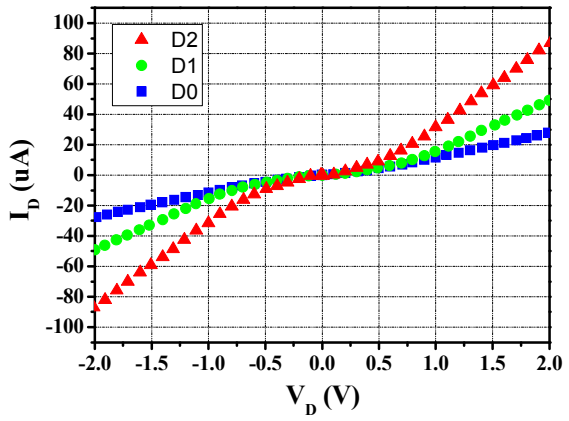

Figure 5. I/V curves of D1 (circles), D2 (triangles), D0 (squares) devices, performed under UV irradiation (λ=365 nm, P_{UV} = 8 W/cm^2) in nitrogen stream (200 sccm).

During the material characterization in the presence of hydrogen stream, we have fixed to 1 Volt the voltage across the devices to work in the linear region. In Figure 6 the device dynamic responses during the exposure to hydrogen are shown. The device response has been reported as percentage of relative current variation calculated as: $(I-I_0)\times100 / I_0 = \Delta I/I_0$ (%) where I_0 was the measured current in nitrogen atmosphere. As reported in literature titania shows n-type semiconducting properties due to presence of donor-type defects (oxygen vacancies and titanium interstitials).[73,74] Several supported metals, and among others Pt, have been studied in order to understand the spilt-over hydrogen species and the nature of activated species.[75,76] Although recent theoretical studies have predicted the weakening of the binding H_2-Pt, during photoexcitation process, there is still a sufficient interaction, which allows the device to be sensitive to hydrogen.[75] In fact, it is possible to assume that a synergic role of titania and Pt allows the hybrid Pt-TiO_2 system to be able to dissociate gaseous hydrogen in to atomic form, contributing to the n-type conductivity enhancement. Figure 6a depicts the comparison between the device responses during an exposure cycle to 700 ppm of hydrogen lasting 120 s and followed by a cleaning to recover the initial condition (I_0). As clearly shown by the curves, the presence of nanostructured platinum on the fiber surface enhances the response of the material to hydrogen and then its sensitivity. The Pt electrodes concur to the hydrogen catalysis but their contribution to the overall device response is lower than that of Pt nanoparticles.

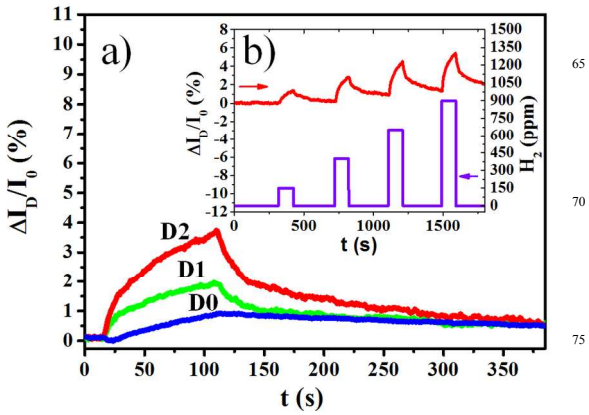

Figure 6. Dynamic response during hydrogen exposure performed under UV irradiation (λ=365 nm, PUV = 8 W/cm^2). (a) Dynamic response of D0, D1 and D2 during exposure to 700 ppm of hydrogen. The insert graph (b) shows the response of D2 device during exposure to increasing concentrations of hydrogen. The exposition to the gas was interrupted after 120 s with a following cleaning procedure performed with dry nitrogen for 360 s.

We observed that platinum nanoparticles have an effect on the dynamic behaviour of the absorption and desorption processes. The dynamic response of D1 and D2, during hydrogen absorption phase, is dominated by two main concurrent phenomena with two different time constants. The first one (tens of seconds) could be related to the hydrogen absorption on PtNPs. The second one (few minutes) could be related to the ionic titanium-hydride bonds formation after dissociation at surface defect sites. This time constant is comparable with the dynamic characteristic of the undecorated device (D0) response.[77]

Figure 6a, highlights that an increasing of PtNPs concentration decreases the response time constant. In similar way, during the cleaning procedure, it is possible to distinguish two main concurrent phenomena related to the hydrogen desorption.

In Figure 6b an example of dynamic response of D2 in presence of different cycles of hydrogen at increasing concentration (150, 400, 650 and 900 ppm) is depicted. The responses versus hydrogen in terms of percentage of relative current variation, is reported in Figure 7.

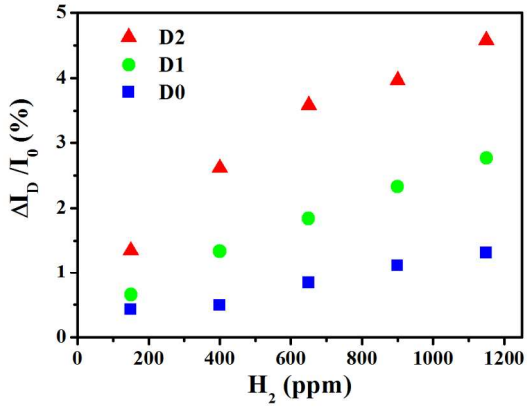

Figure 7. Response curve of D1 (circles), D2 (triangles), D0 (squares) devices versus hydrogen concentrations.

It is possible to observe that the investigated devices show an increasing sensitivity due to platinum nanoparticles concentration; increasing the PtNPs quantity, an increase of the response was observed. Device D2 exhibits a response at least two times higher than D1 and four times higher than D0.

Defining the limit of detection (LOD) as three times of the noise value and evaluating the response noise as 0.2%, we have obtained 75 ppm of LOD for hydrogen. It should be pointed out that the presence of PtNPs on the surface of TiO_2-NFs allowed to observe an increased response towards hydrogen gas at concentration in the range 100-1150 ppm, under UV irradiation and at room temperature, with an enhancement of photoconductivity and dynamic performance. In particular the performances at room temperature is noteworthy in comparison with literature reports and the main advantages is in the simple synthesis process, low cost and especially the better mechanical stability that make it more commercially available for room-temperature hydrogen sensing devices.[78,79,32] For example, Pt/Nb_2O_5 hydrogen sensor, composed by a pair of platinum electrodes deposited on the surface of the Nb_2O_5 NW membrane, was investigated at room temperature and exhibited a sensitive hydrogen response (100-2000 ppm), with response time of 240-250 s.[79] Also an indium doped SnO_2 MEMS device, with Au electrodes, has been reported to allow hydrogen detection at room temperature (900 ppm) with a response time of 250–350 s.[80]

4. Conclusions

In summary, we report the synthesis and characterization of Pt-3MPS nanoparticles, with diameters in the range of 5-10 nm and high stability in water solution, as confirmed by ζ-potential values. New hybrids, based on electrospun TiO_2-NFs decorated by Pt-NPs, were prepared by a simple and readily scalable up procedure. These materials have been studied for H_2 sensors development, showing combined properties of TiO_2 photoconduction and Pt sensitivity and low temperature response improved with respect to that of undecorated TiO_2-NFs. In fact, Pt-TiO_2 investigated as sensing material towards hydrogen gas in the range 100-1150 ppm (at room temperature under UV irradiation) shows enhancement of phoconductivity (150%), high response (400%) and an advance on dynamic performances. Our results point out that the new hybrids can be extremely versatile and foresee the improvement of hydrogen sensors based on nanostructured materials.

Acknowledgment

We gratefully acknowledge the Sapienza University of Rome, Ateneo Sapienza 2013/C26A13HRZ4 project, for financial support. Ilaria Fratoddi acknowledges the Dept. of Chemistry, Sapienza University of Rome, for Support Research Initiative. A special thank to Professor C. Cametti for his kind help.

Notes and references

[a] *Department of Chemistry, University of Rome Sapiens, P.le A. Moro 5, I-00185 Rome, Italy E-mail: iole.venditti@uniroma1.it*
[b] *Center for Nanotechnology for Engineering (CNIS), University of Rome Sapienza, P.le A. Moro 5, I-00185 Rome, Italy*
[c] *CNR-Institute of Atmospheric Pollution Research, V. Salaria Km 29,300, Monterotondo, 00015 Rome, Italy, E-mail: e.zampetti@iia.cnr.it*
[d] *Department of Physics, Unita INSTM and CISDiC University Roma Tre, Via della Vasca Navale 85, 00146 Rome, Italy*
[e] *Center for Protection of Environment and Cultural Heritages (CIABC) Sapienza University of Rome, P.le A. Moro 5, 00185 Rome, Italy*
† Electronic Supplementary Information (ESI) available. See DOI: 10.1039/b000000x/

[1] M. K. Debe, *Nature* 2012, **486**, 43
[2] M. Graetzel, R. A. J. Janssen, D. B. Mitzi, E. H. Sargent *Nature* 2012, **488**, 304
[3] I. Venditti, N. Barbero, M. Russo, A. Di Carlo, F. Decker, I. Fratoddi, C. Barolo and D. Dini, *Materials Research Express* 2014,**1**,015040
[4] I. Fratoddi, E.S. Bronze-Uhle, A. Batagin-Neto, D. M. Fernandes, E. Bodo, C. Battocchio, I. Venditti, F. Decker, M. V. Russo, G. Polzonetti, C. F. O. Graeff, *J. Phys. Chem. A* 2012, **116**, 8768
[5] A. Batagin-Neto, E.S. Bronze-Uhle, D.M. Fernandes, I. Fratoddi, I. Venditti, F. Decker, E. Bodo, M.V. Russo, C.F.O. Graeff, *J. Phys. Chem. B* 2011, **115**, 8047
[6] R. De Angelis, I. Venditti, I. Fratoddi, F. De Matteis, P. Prosposito, I. Cacciotti, L. D'Amico, F. Nanni, A. Yadav, M. Casalboni, M. V. Russo, *J. Colloid Interface Sci.,* 2014, **414**, 24
[7] S. Schutzmann, I. Venditti, P. Prosposito, M. Casalboni, M.V. Russo; *Optics Expres*, 2008, **16,** 897
[8] R. D'Amato, L. Medei, I. Venditti, M. V. Russo, M. Falconieri; *Mat. Sci. Eng. C*, 2003, **23**, 861
[9] I. Fratoddi, I. Venditti, C. Cametti, C. Palocci, L. Chronopoulou, M. Marino, F. Acconcia and M.V. Russo, *Colloids and Surfaces B: Biointerfaces* 2012, **93**, 59
[10] A. Laganà, I. Venditti, I. Fratoddi, A.L. Capriotti, G. Caruso, C. Battocchio, G. Polzonetti, F. Acconcia, M. Marino and M.V. Russo, *J. Colloid Interface Sci.,* 2011, **361**, 465
[11] I. Fratoddi, I. Venditti, C. Cametti, M.V. Russo; *J. Mater. Chem. B* 2014 DOI: 10.1039/C4TB00383G
[12] A. Devadoss, P. Sudhagar, S. Das, S. Yun Lee, C. Terashima, K. Nakata, A. Fujishima, W. Choi, YS. Kang, U. Paik, *ACS Appl. Mater. Interfaces*, 2014, **6,** 4864
[13] I. Venditti, I. Fratoddi, MV Russo and A. Bearzotti, *Nanotechnology* 2013, **24**, 155503
[14] A. Bearzotti, A. Macagnano, S. Pantalei, E. Zampetti, I. Venditti, I. Fratoddi, M.V. Russo; *J. Phys.: Condens. Matter* 2008, **20**, 474207
[15] E. Zampetti, S. Pantalei, S. Scalese, A. Bearzotti, F. De Cesare, C. Spinella, A. Macagnano,. (2011) *Biosensors and Bioelectronics*, 2010, **26**, 2460

[16] Samuel E Lohse, Nathan D. Burrows, Leonardo Scarabelli, Luis M. Liz-Marzan, and Catherine Jones Murphy *Chem. Mater.*, 2014, **26**, 34
[17] I. Fratoddi, I. Venditti, C. Battocchio, G. Polzonetti, F. Bondino, M. Malvestuto, E. Piscopiello, L. Tapfer; M.V. Russo; *J. Phys. Chem. C* 2012, **115**, 15198
[18] C. Caliendo, G. Contini, I. Fratoddi, S. Irrera, P. Pertici, G. Scavia, M.V. Russo*, Nanotechnology* 2007, **18**, 125504
[19] R P Kurta, L Grodd, E Mikayelyan, O Y Gorobtsov, I Fratoddi, I Venditti, M Sprung, S Grigorian, I A Vartanyants; J. Phys.: Conference Series 2014, **499**, 012021
[20] H.-Y. Lai, C.-H. Chen, *J. Mat. Chem.* 2012, **22**, 13204
[21] C. Zhang, A-F Kanta, H. Yin, A. Boudiba, J. D'Haen, M-G Olivier, M. Debliquy, *Int.J.Hydrogen Energy* 2013, **38**, 2929
[22] T-L Hsieh, H-W Chen, C-W Kung, C-C Wang, R. Vittala, K-C Ho *J. Mater. Chem.*, 2012, **22**, 5550
[23] N. Barsan, D. Koziej, U. Weimar, *Sens. Actuators B*, 2007, **121**, 18
[24] O.K. Varghese, D. Gong, M. Paulose,K.G. Ong, C.A. Grimes *Sens. Actuators B* 2003, **9**, 338
[25] G.K.Mor, M.A. Corvalho, O.K. Varghese, M.V. Pishko, C.A.Grimes, *J.Mat.Res.,*2004, **19**, 628
[26] S.K.Arya, S.Krishnan, H.Silva, S.Jean, S.Bhansali, *Analyst,* 2012, **137,** 2743
[27] Q. Xiang, G. Meng, Y. Zhang, J. Xu, P. Xu, Q. Pan,W. Yu, *Sens. Actuators B*, 2010, **143**, 635
[28] X. Liu, J. Zhang, X. Guo, S. Wu and S. Wang, *Nanoscale*, 2010, **2**, 1178
[29] Y. H. Lin, Y. C. Hsueh, P. S. Lee, C. C. Wang, J. M. Wu, T. P. Perng, H. C. Shih, *J. Mater. Chem*., 2011, **21**, 10552;
[30] H. T. Wang, B. S. Kang, F. Ren, L. C. Tien, P. W. Sadik, D. P. Norton, S. J. Pearton, Jenshan Lin, *Appl.Phys.Lett.,* 2005, **86**, 243503
[31] X. Xue, Z. Chen, C. Ma, L. Xing, Y. Chen, Y. Wang, T. Wang, J. *Phys. Chem. C*, 2010, **114**, 3968
[32] B. Liu, D. Cai, Y. Liu, H. Li, C. Weng, G. Zeng, Q. Li, T. Wang *Nanoscale*, 2013, **5**, 2505
[33] J. Kukkola, M. Mohl, A-R. Leino, J.Maklin, N.Halonen, A. Shchukarev, Z. Konya, H.Jantunen, K.Kordas, *Sens. Actuators B,* 2013, **186**, 90
[34] X. Pan, M-Q Yang, X. Fu, N. Zhang, Y-J Xu *Nanoscale*, 2013, **5**, 3601
[35] S. Liu, J. J. Hu, N. F. Yan, G. L. Pan, G. R. Li, X. P. Gao, *Energy Environ. Sci.,* 2012, **5**, 9743
[36] W. Wang, M. Tian, A. Abdulagatov, S. M. George, Y.-C. Lee R. Yang, *Nano Lett*., 2011, **12**, 655
[37] E. Zampetti, S. Pantalei, A. Muzyczuk, A. Bearzotti, F. De Cesare, C. Spinella, A. Macagnano, *Sens. Actuators B* 2013, **176**, 390
[38] E. Zampetti, A. Magagnano and A. Bearzotti, *J Nanopart Res.,* 2013, **15**, 1566
[39] X. Chen, S.S. Mao, *Chem. Rev.* 2007,**107**,2891
[40] G. Zhang, H. Duan, B. Lu, Z. Xu *Nanoscale*, 2013, **5**, 5801
[41] L. Zhao, Y.-S. Hu, H. Li, Z. Wang and L. Chen, *Adv. Mater*.,**2011**, 23, 1385
[42] V. Etacheri, R. Marom, R. Elazari, G. Salitra, D. Aurbach, *Energy Environ. Sci.*, 2011, **4**, 3243
[43] S. Ramakrishna, K. Fujihara, W.E. Teo, T. Yong, Ma Zuwei, R. Ramakrishna *Materials Today* 2006, **9**, 40
[44] A. Macagnano, E., Zampetti, S. Pantalei, F. De Cesare, A. Bearzotti, K.C. Persaud, *Thin Solid Films* 2011, **520**, 978
[45] D. Li, Y. Xia, *Nano Letters* 2003, **3**, 555
[46] J. Watthanaarun, V. Pavarajarn, P. Supaphol, *Science and Technology of Advanced Materials*, 2005, **6,** 240
[47] C.L Lawson and I.D. Morrison, I.D. Solving least squares problems. A FORTRAN program and subroutines called NNLS, Prentice-Hall, Englewood Cliffs, NJ 1974
[48] S.W. Provencher, *Comput. Phys. Commun*. 1982, **27**, 213
[49] I. Fratoddi, I. Venditti, C. Battocchio, G. Polzonetti, C. Cametti, M.V. Russo, *Nanoscale Res. Lett.* 2011, **6**, 98
[50] I. Venditti, I. Fratoddi, C. Battocchio, G. Polzonetti, C. Cametti, M.V. Russo, *Polym. Int.* 2011, **60**, 1222
[51] R. D'Amato, L. Medei, I. Venditti, M. V. Russo, M. Falconieri, *Mat. Sci.Eng. C* 2003, **23,** 861
[52] C. Cametti, I. Fratoddi, I. Venditti, M. V. Russo; *Langmuir* 2011, **27**, 7084
[53] H. Ohshima and K. Furusawa K. Electrical Phenomena at Interfaces, second ed., Dekker, NY, 1998
[54] P. Swift, D. Shuttleworth, M.P. Seah, *Practical Surface Analysis by Auger and X-ray Photoelectron Spectroscopy*, D. Briggs and M. P. Seah (Eds.), J. Wiley & Sons, Chichester, 1983, chapter 5 and appendix 3
[55] D.A. Shirley, *Phys. Rev. B*, 1972, **5**, 4709
[56] I. Venditti, I. Fratoddi and A. Bearzotti, *Nanotechnology* 2010, **21**, 355502
[57] I. Fratoddi, P. Altamura, A. Bearzotti, A. Furlani, M.V. Russo, *Thin Solid Films*, 2004, **458**, 292
[58] I. Venditti, R. D'Amato, M. V. Russo and M. Falconieri, *Sens. Actuators B* 2007, **126,** 35
[59] I. Venditti, I. Fratoddi, C. Palazzesi, P. Prosposito, M. Casalboni, C. Cametti, C. Battocchio, G. Polzonetti and M. V. Russo, *J. Colloid Interface Sci.,* 2010, **348**, 424
[60] I.D. Morrison, S. Ross, Colloidal dispersions: suspensions, emulsions, and foams. Wiley-Interscience, New York 2002
[61] S.K Mehta, S. Kumarnd M. Gradzielski, *J. Colloid Interface Sci.,* 2011, **360**, 497
[62] C. Yee, M. Scotti, A. Ulman, H. White, M. Rafailovich and J. Sokolov, *Langmuir* 1999, **15**, 4314
[63] F. A. Lewis, The Palladium-Hydrogen System (Academic, London and New York, 1967).
[64] A.Abburi, W.J.Yeh, *IEEE Sensors Journal,* 2012, **12**, 2625
[65] A.Kaniyoor, R.Imran Jafri, T.Arockiadoss, S.Ramaprabhu, *Nanoscale,* 2009, **1**, 382
[66] P.A. Russo, N. Donato, S.G. Leonardi, S. Baek, D.E. Conte, G. Neri, N. Pinna, *Angew Chem Int Ed Engl.* 2012, **51**, 11053
[67] NIST X-ray Photoelectron Spectroscopy Database, Version 4.1 (National Institute of Standards and Technology, Gaithersburg, 2012); http://srdata.nist.gov/xps/.]
[68] M. Quintiliani, M. Bassetti, C. Pasquini, C. Battocchio, M. Rossi, F. Mura, R. Matassa, L. Fontana,MV Russo, I. Fratoddi, *J. Mater. Chem. C*, 2014, Advance Article DOI: 10.1039/C3TC32567A
[69] C. Battocchio, C. Meneghini, I. Fratoddi, I. Venditti, MV. Russo, G. Aquilanti, C. Maurizio, F. Bondino, S. Mobilio, G. Polzonetti; *J. Phys. Chem. C*, 2012, **116**, 19571
[70] I.Venditti, L. Fontana, I. Fratoddi, C. Battocchio, C. Cametti, S. Sennato, F. Mura, F. Sciubba, M. Delfini and M.V. Russo, *J. Colloid Interface Sci.,* 2014, **418**, 52
[71] S.K. Kim, G-J Choi, S.Y. Lee, M. Seo, S.W. Lee, J.H. Han, H-S Ahn, S. Han, C.S. Hwang, *Adv. Mater.*2008, **20,** 1429
[72] W.Y. Park, G.H. Kim, J.Y. Seok, K.M. Kim, S.J. Song, M.H. Lee, C.S. Hwang, *Nanotechnology* 2010, **21**, 195201(4pp)
[73] R.N. Blumenthal, J. Baukus, W.M. Hirthe, *J Electrochem Soc*, 1967, **114**, 172
[74] J. Nowotny, T. Bak, M.K. Nowotny, L.R. Sheppard, *Int J Hydrogen Energy*, 2007, **32**, 2630
[75] A. Boonchun, N. Umezawa, T. Ohno, S. Ouyang, J. Ye, *J. Mater. Chem. A,* 2013, **1**,6664
[76] U. Roland, T. Braunschweig, F. Roessner, *J. Mol. Cat. A: Chem.* 1997, **127,** 61-84
[77] W. Gopel, G. Rocker, R. Feierabend, *Phys.Rev. B* 1983, **28**, 3427 .
[78] V. Kumar, Sunny, I. Rawal, V.N. Mishra, R. Dwivedi, R.R. Das, *Mat. Chem. Phys.,*2014, **146**, 418
[79] Z. Wang, Y. Hu, W. Wang, X. Zhang, B. Wang, H. Tian, Y. Wang, J. Guan, H. Gu, *Int. J. Hydrogen Energy*, 2012, **37**, 4526
[80] S. Shukla, P. Zhang, H.J. Cho, S. Seal, L. Ludwig, *Sens. Actuators B,* 2007, **120,** 573